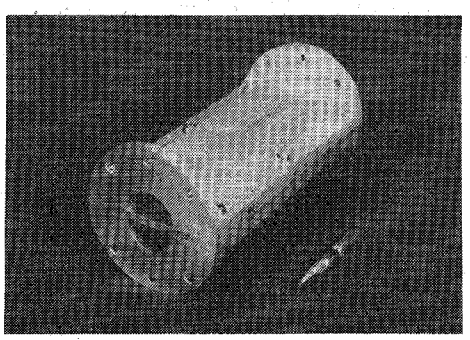

Fig. 4. Trial multiple branch-guide 3-dB directional coupler.

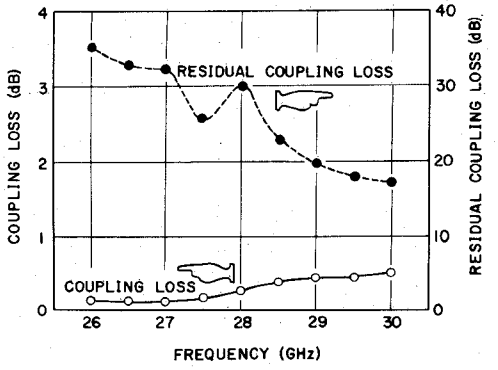

Fig. 5. Measured frequency responses of the 0-dB coupler (44 branches).

It was suspected that mode conversion may occur because the TE_{01}-mode semicircular waveguide is an overmoded waveguide. Especially, the TE_{21} mode may propagate because the propagation-constant difference between the TE_{21} mode and the TE_{01} mode is very small, and because the field distribution of the TE_{21} mode at the plane wall is similar to that of the TE_{01} mode. The mode-conversion ratio of the TE_{21} mode was experimentally measured using a tapered semicircular TE_{21}-mode transducer [5]. It was found that the mode-conversion ratio was less than -20 dB, the conversion loss is less than 0.05 dB, and the mode conversion of the TE_{21} mode has a negligible effect on the TE_{01} mode.

Conclusion

Design parameters of the present approximate theory have made it possible to construct multiple branch-guide directional couplers using a TE_{01}-mode semicircular waveguide. Since the length of the 0-dB coupler for the experimental model is about 150 mm, which is shorter than the conventional coupled wave-type 0-dB coupler, the insertion loss is proportionally decreased. It is possible to make a more compact diplexer and to decrease the insertion loss of the diplexer for the millimeter-wave band and also for the 20–30-GHz band.

It is expected that the technique will be used in the band-splitting filter for the 30-GHz band in the earth station of the Japanese domestic satellite communication system [6].

Acknowledgment

The author wishes to thank M. Shinji and Dr. I. Ohtomo for their constant encouragement.

References

[1] S. Shimada and N. Suzuki, "Semicircular waveguide-type diplexer used for the millimeter-wave waveguide transmission system," *IEEE Trans. Microwave Theory and Tech.*, vol. MTT-22, pp. 111–118, Feb. 1974.
[2] J. Reed, "The multiple branch waveguide coupler," *IRE Trans. Microwave Theory and Tech.*, vol. MTT-6, pp. 398–403, Oct. 1958.
[3] ——, "Branch waveguide coupler design charts," *Microwave J.*, pp. 103–104, Jan. 1963.
[4] S. Iiguchi, "Mode conversion in the excitation of TE_{01} wave in a TE_{01} taper type mode transducer," *Elec. Commun. Tech. J.*, Nippon Telegraph and Telephone Public Corp., Japan, vol. 11, pp. 319–325, Nov. 1962.
[5] N. Nakajima, "A wide band tapered type semicircular TE_{21} mode transducer," *Trans. Inst. Electron. Commun. Eng. Japan*, vol. 57B, pp. 194–195, Mar. 1974.
[6] F. Ikegami and S. Morimoto, "Plans for the Japanese domestic satellite communication system," 1972 IEEE INTERCON.

A Frequency-Independent Large-Signal Equivalent Circuit for a BARITT Diode and Its Application to an Amplifier

KAORU OKAZAKI, MEMBER, IEEE,
NION SOCK CHANG, MEMBER, IEEE, AND
YUKITO MATSUO

***Abstract*—A frequency-independent large-signal equivalent circuit having five elements with only one resistive element is presented for the BARITT diode. It is valid over the useful frequency range and is used for the investigation of the BARITT-diode amplifier.**

Introduction

The terminal characteristics of a microwave negative-resistance device are nonlinear. An equivalent-circuit representation [1] of the device, especially a frequency-independent equivalent circuit, is useful in the investigation of the device performance in a practical microwave circuit.

Recently, a large-signal frequency-independent equivalent circuit has been proposed for IMPATT-diode characterization by Gupta [2]. Although this equivalent circuit permits a useful frequency range of validity, it requires a complex process for evaluating the circuit elements and has a disadvantage in application to the amplifier design because of two or three resistive elements in the circuit [3]. The purpose of this short paper is to present a novel frequency-independent large-signal equivalent circuit having only one resistive element for a BARITT diode and an application to the investigation of a BARITT-diode amplifier performance.

Evaluation of the Equivalent Circuit

The frequency-independent equivalent circuit proposed here is shown in Fig. 1. The basic circuits of the equivalent circuit are a series resonant circuit with a negative resistance and a shunt resonant circuit. The admittance of the equivalent circuit $Y_{eq}(\omega)$ is

$$Y_{eq}(\omega) = \frac{R}{R^2 + [\omega L_s\{1 - (\omega_s/\omega)^2\}]^2} + j\left[\omega C_p\{1 - (\omega_p/\omega)^2\} - \frac{\omega L_s\{1 - (\omega_s/\omega)^2\}}{R^2 + [\omega L_s\{1 - (\omega_s/\omega)^2\}]^2}\right] \quad (1)$$

where $\omega_s = (\sqrt{L_s \cdot C_s})^{-1}$ and $\omega_p = (\sqrt{L_p \cdot C_p})^{-1}$.

Manuscript received May 27, 1975; revised May 29, 1975.
The authors are with the Institute of Scientific and Industrial Research, Osaka University, Osaka 565, Japan.

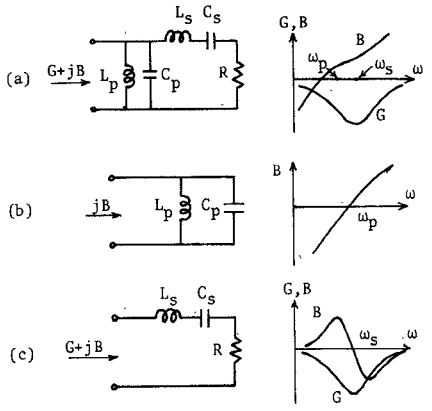

Fig. 1. Frequency-independent equivalent circuit (a), its basic circuits (b), (c) and their admittances.

TABLE I
PARAMETERS OF THE EQUIVALENT CIRCUIT

	a	b	c	
R^{-1}	-1.261 mmho		0.0294	v^{-2}
L_s	26.51 nH	0.0386 v^{-1}	0.0353	
C_s	0.0087 pF	-0.093	0.0012	
L_p	1.778 nH	-0.0996	0.0590	
C_p	0.517 pF	-0.0021	-0.0022	

Parameters are defined in eq.(2) for L_s, C_s, L_p, C_p.
The resistance is expressed by $R^{-1}=a\cdot\exp(-c\cdot Vrf^2)$.

A method for determining the equivalent circuit for a diode admittance, which may have been determined experimentally or by an analysis, is the following. First, the conductance of the equivalent circuit should be fitted to that of the diode by selecting the elements of the series resonant circuit, then the elements of the shunt resonant circuit are selected to yield the susceptance of the equivalent circuit closely agreeing with the diode susceptance. The large-signal behavior can be incorporated in the equivalent circuit by expressing the elements as frequency-independent functions of the RF voltage across the diode, particularly quadratic functions of the form

$$f(V_{RF}) = a(1 + bV_{RF} + cV_{RF}^2) \tag{2}$$

where V_{RF} is the amplitude of the RF voltage and a,b,c are constants. Large-signal admittance curves of the diode are similar to the small-signal admittance curve, and therefore sets of elements for various V_{RF} are determined in the same way in the small-signal case. Using these data of "elements versus V_{RF}," finally, 14 or 15 unknowns can be determined from (2), Table I.

The admittance of the equivalent circuit for a BARITT diode is given in Fig. 2, where the diode admittance has been given by the large-signal analysis in [4]. It can be seen that a good agreement between the diode and equivalent-circuit large-signal admittance is possible over a useful frequency range.

Application to a BARITT-Diode Amplifier

In this part, the large-signal equivalent circuit of a BARITT diode will be used to investigate the performance of a BARITT-diode amplifier for a typical circulator-coupled reflection-type circuit as shown in Fig. 3(a). It will be assumed that the diode is the X-band Si-BARITT diode for which an equivalent circuit

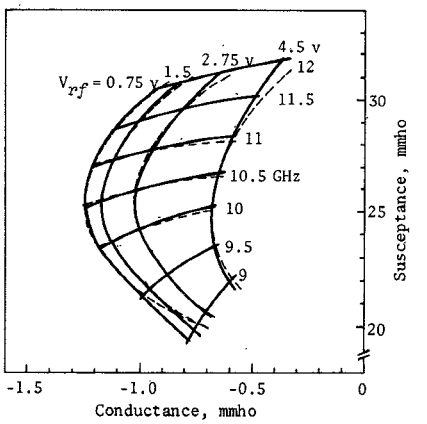

Fig. 2. Large-signal admittances of a BARITT diode and of the equivalent circuit. Parameters are listed in Table I. – – – diode, —— equivalent circuit.

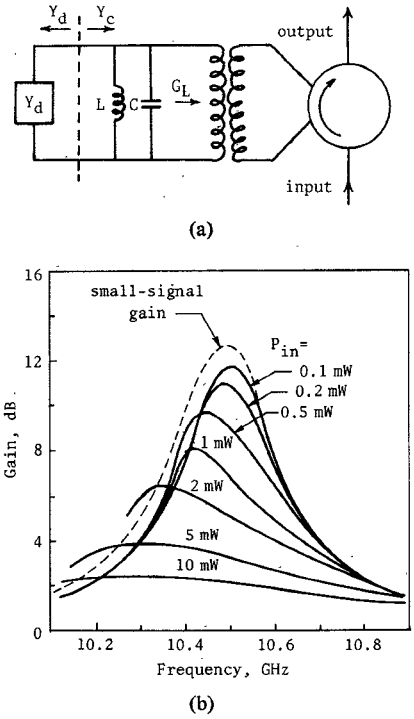

Fig. 3. (a) Schematic diagram of a circulator-coupled reflection-type BARITT-diode amplifier and (b) its calculated frequency response at different input power levels. G_L = 2 m℧, $Q_c = 2\pi f_c \cdot C/G_L$ = 10, $f_c = (2\pi\sqrt{LC})^{-1}$ = 19.03 GHz.

has been found in Fig. 2. The power gain of a reflection-type amplifier is given by

$$G = \left|\frac{Y_c - Y_d^*}{Y_c + Y_d}\right|^2 \tag{3}$$

where the asterisk denotes the complex conjugate and Y_c and Y_d are the circuit and device admittances as seen at some arbitrarily chosen reference plane, looking away from and towards the device, respectively. With a sinusoidal voltage across the diode, the RF-power added by the amplifier is given by

$$P_{add} = \tfrac{1}{2}|G_d|V_{RF}^2 \tag{4}$$

and the output power is

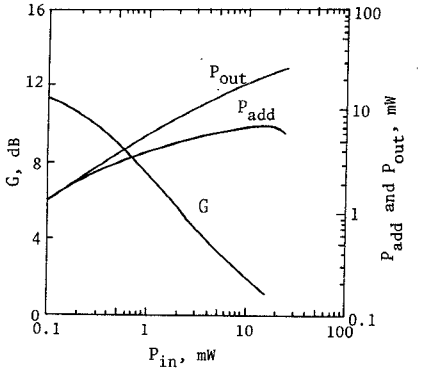

Fig. 4. Variations of gain, output power, and added power with input power at a single operating frequency, 10.5 GHz.

$$P_{out} = G \cdot P_{in} = P_{in} + P_{add}. \quad (5)$$

Fig. 3(b) shows the calculated amplifier frequency response. Here, the reference plane was chosen at the terminals of the diode chip, therefore $Y_d = Y_{eq}$ in (3). For the circuit admittance Y_c, a single-tuned circuit was assumed and the package parasitics were omitted. [Including the package parasitics, such as a pill-prong-type package, the bandwidth of the amplifier was almost equal to that in Fig. 3(b).] The small-signal power gain and the bandwidth at 3-dB down are obtained to be 12.7 dB and 270 MHz, respectively. As the input level is increased, the gain compression occurs and the bandwidth of the amplifier becomes wider as observed in our experimental results [5]. The gain expansion at lower frequencies can be seen, because the susceptance of the diode becomes large with increasing input signal level. It can also be seen that the gain compression with an increasing input level is severe at frequencies where the small-signal gain is high. The variations of power gain, power added, and power output with input power are shown in Fig. 4 at a single operating frequency. The added power reaches a maximum value and falls upon further increasing input power and the saturation of output power and gain compression occur as observed experimentally.

Conclusion

A frequency-independent large-signal equivalent circuit has been proposed for a BARITT diode and is shown to be well applicable to the investigation of the device performance in a practical microwave circuit. This equivalent circuit has only one resistive element. Therefore, the equivalent circuit of our model will be useful for an optimum design of an amplifier for a small-signal case because the reference plane can be chosen at the terminals of this resistive element so that Y_c consists of linear passive elements only.

The equivalent circuit proposed here for a BARITT diode will be applicable to other active devices such as IMPATT's.

References

[1] M. E. Hines, "Negative resistance diode power amplification," *IEEE Trans. Electron Devices*, vol. ED-17, pp. 1–8, 1970.
[2] M. S. Gupta, "Large-signal equivalent circuit for IMPATT-diode characterization and its application to amplifiers," *IEEE Trans. Microwave Theory and Tech.*, vol. MTT-21, pp. 689–694, 1973.
[3] H. W. Bode, "Network analysis and feedback amplifier design."
[4] M. Matsumura, "Large-signal analysis of silicon BARITT diodes," *Electronics and Communications in Japan*, vol. 56, no. 5, pp. 35–36, 1973.
[5] K. Okazaki, N. S. Chang, and Y. Matsuo, "Experimental studies on the large-signal operation of the BARITT-diode amplifiers," *Electronics and Communications in Japan*, vol. 58, no. 5, pp. 29–30, 1975.

High-Quality Image Reconstruction from Double Microwave Holograms

HIROSHI SHIGESAWA, MEMBER, IEEE,
KEI TAKIYAMA, MEMBER, IEEE, AND
MAMPEI NISHIMURA

***Abstract*—A new mode of microwave holography is described. This is based upon the simultaneous deconvolution applied to double holograms obtained at different positions in space and has produced markedly improved microwave images. The effectiveness of the present method is demonstrated in both simulations and experiments.**

The technique of microwave holography [1], [2] is of considerable importance for imaging objects obscured by media which are optically opaque but are transparent to microwaves. However, microwave holograms usually have small apertures in terms of the recording wavelength, and thus resolution is severely restricted and the quality of reconstructed images is often poor. In a previous paper [3], a successful application of digital image enhancement was demonstrated to restore the degraded quality of image without recourse to knowledge of the degrading phenomena. However, the image from a microwave hologram suffers from two inherent degradations resulting from the fact that: 1) the hologram data are really a convolution of the correct data with the radiation characteristics of a microwave radiator; and 2) the reconstructed true image is accompanied with a noisy conjugate image in the case of Gabor holograms. To eliminate these unwanted effects,[1] a new mode of holography is demonstrated in this short paper. This technique is based upon the simultaneous deconvolution applied to double holograms obtained at different positions in space and its essence is understood from ordinary holography which is based upon the simultaneous transmitter–receiver-scanned hologram scheme [5] shown in Fig. 1. For simplicity we assume that the object exists on the x_0 axis with a complex reflection function $\sigma(x_0)$. Let a small broad-beam antenna having a directivity $w(\theta)$ in the x–y plane scan on the x axis, while the object is illuminated with CW microwave energy radiated from a sequence of positions along the scanning axis. Here we consider two kinds of holograms that would be obtained on the x_1 and x_2 axes which are parallel to each other. The distance between the x_0 and x_m axes is assumed as y_{0m} ($m = 1,2$). When the returned signal to the antenna from the object is coherently detected with the transmitting wave, the detected signal denoted by $\tilde{h}(x,y_{0m})$ may be expressed with the convolution integrals as follows:

$$\tilde{h}(x,y_{0m}) = a_m[\exp(j\phi_m)\sigma(x) \circledast t(x,y_{0m}) + \exp(-j\phi_m)\sigma^*(x) \circledast t^*(x,y_{0m})], \quad m = 1,2 \quad (1)$$

where $\circledast$ denotes the convolution integral, the asterisk means the complex conjugate, and ϕ_m denotes the constant phase difference between the returned signal and the internal reference wave. In the paraxial approximation, the system propagator

Manuscript received October 17, 1975; revised January 12, 1976.
H. Shigesawa and K. Takiyama are with Doshisha University, Kyoto, Japan.
M. Nishimura is with Maizuru Technical College, Maizuru, Japan.

[1] The possibility of eliminating the conjugate image in a Gabor hologram has been previously suggested by Bragg and Rogers [4] in the field of diffraction microscopy. However, the technique used here is different.